

## THERMOGRAVIMETRIC ANALYSIS, OPTICAL AND DIELECTRIC PROPERTIES OF NEWLY DEVELOPED $\text{LiNi}_{0.5}\text{Pr}_x\text{Fe}_{2-x}\text{O}_4$ NANOCRYSTALLINE FERRITES

Z. A. GILANI<sup>a,\*</sup>, M. S. SHIFA<sup>c</sup>, A. D. CHANDIO<sup>f</sup>, M. N. USMANI<sup>b</sup>,  
H. M. N. UL HUDA K. ASGHAR<sup>a</sup>, S. ASLAM<sup>a</sup>, M. KHALID<sup>a</sup>, A. PERVEEN<sup>a</sup>,  
J. UR REHMAN<sup>a</sup>, M. MUSTAQEEM<sup>e</sup>, M. A. KHAN<sup>d</sup>

<sup>a</sup>*Department of Physics, Balochistan University of Information Technology, Engineering & Management Sciences, Quetta 87300, Pakistan*

<sup>b</sup>*Department of Physics, Bahauddin Zakariya University, Multan, Pakistan*

<sup>c</sup>*Department of Physics, Government College University Faisalabad, 38000, Pakistan*

<sup>d</sup>*Department of Physics, The Islamia University of Bahawalpur, Bahawalpur-63100, Pakistan*

<sup>e</sup>*Department of Chemistry, The Islamia University of Bahawalpur, Bahawalpur-63100, Pakistan*

<sup>f</sup>*Department of Metallurgical Engineering, NED University of Engineering and Technology, Karachi, 75270, Pakistan.*

A series consisting of six samples of  $\text{Li}_{0.5}\text{Ni}_{0.5}\text{Pr}_x\text{Fe}_{2-x}\text{O}_4$  spinel ferrites with different molar concentrations have been fabricated by using facile micro-emulsion method. Studies like TGA/DTA, Fourier transform infrared spectroscopy (FTIR), dielectric properties were employed to see the result of praseodymium doping on structural, optical and dielectric factors. TGA graph elucidates the decrease in weight as temperatures rise but this weight loss becomes smooth after 800 °C and limits at 950 C, hence no further weight loss. Single phase formation is confirmed at this temperature range. The FTIR spectroscopy inveterate the intrinsic cation vibrations of metal ions of the spinel structure, these are found between 400 and 1000  $\text{cm}^{-1}$ . The dielectric studies are carried out between ranges of 1MHz to 3GHz frequency of the applied electric field. The dielectric parameters deceased by praseodymium substitutions. Moreover, a decreasing effect is also seen by the increasing the frequency. This kind of domino effects in dielectric parameters indicates the use of these nanocrystalline ferrites in the synthesis of microwave devices. The devices made by this kind of materials will be operated at GHz frequencies ranges.

(Received May 29, 2018; Accepted September 8, 2018)

**Keywords:** Li-Pr, Praseodymium, Nanocrystalline ferrites, TGA, Microemulsion, Dielectric parameters

### 1. Introduction

Studies in nanotechnology have focused the attention of scientists towards doping of rare earth metal nano-crystals owing to their vast applications. Nanocrystalline ferrites doped with rare earth metals have physical and technological applications [1]. Lithium-based rare earth metal doped ferrites are a type of magnetic materials that have a greater value of dielectric parameters[2]. Moreover, lithium based ferrites are an inexpensive substitute to garnet based nanomaterials [3] Normally the properties of ferrites lead to the way of synthesis and annealing temperature [4]. However, intrinsic properties of ferrites like the dielectric loss, dielectric constant, conductivity, resistivity and magnetic properties controlled by the type of doping metals and its

---

\*Corresponding authors: zagilani2002@yahoo.com

chemical composition [5, 6]. Intrinsic properties diverge owing to the cation distribution of metal and electron hopping mechanism. Former studies revealed that different rare earth metals doping develop various performances of spinel ferrites [5]. The doping of nickel and rare earth cations along with Fe gave marvelous intrinsic properties [7]. Numerous studies have been done on spinel ferrites to vary the properties with the use of rare earth metal cations in these spinel ferrites [8]. Intrinsic properties are tailored using the concentration of lithium ferrites and dopant materials. Furthermore, rare earth cations having greater ionic radii, which is liable for their properties [9]. Various methods are used to prepare doped lithium ferrites like hydrothermal, co-precipitation, ceramic method, hydrothermal techniques, sol-gel method and micro-emulsion method [8]. Lithium ferrites of rare earth cations have higher ionic radii are mainly liable for electromagnetic properties [9]. Nanocomposite (RE=Nd-Pr) alloys, where they explain that enhanced grain modification was attained through the Nb accumulation, but the magnetic properties were approximately similar to Zr doped alloys [10]. Hao-Xin Mai et al., describe the optical properties of High-Quality Sodium Rare-Earth Fluoride Nanocrystals. They successfully measured the photo luminescent of NaEuF<sub>4</sub> nanocrystals (2006) [11]. Rodriguez-Carvajal et al., describe the neutron diffraction study on structural and magnetic features of La<sub>2</sub>NiO<sub>4</sub> system using neutron experiments. They explain the phase transition using Bragg reflection also studies ferromagnetic components [12]. Ganesh, I et al., synthesized gAl<sub>2</sub>O<sub>3</sub> nanocrystalline using microwave assisted combustion route. The results indicated that with the greater compositional stability and purity of nanocrystalline is found than other combustion techniques [13]. Electrical and dielectric properties of Ni-CO substituted nanocrystalline study Mathe, V. L. et al.,(2008). They explained that varying electrical resistivity as a function of temperature investigated at 300-900 K. The results clearly indicated that four breaks into five regions in that range of temperature. A magnetic transition of temperature determined from resistivity behavior with temperature [14]. Dutta P. et al.,( 2007) study the comparative magnetic properties of bulk Co<sub>3</sub>O<sub>4</sub>nanocrystalline using sol-gel route. They used Neel temperature (T<sub>N</sub>) to determine the magnetic susceptibility vs temperature data of bulk material. They also verify the finite size effects associated with Co<sub>3</sub>O<sub>4</sub> nanoparticles at T<sub>N</sub> = 26K [15].

In our current research, Praseodymium (Pr) is substituted in LiNi-based spinel ferrites develop using microemulsion route and study the impacts of Pr<sup>+3</sup> concentrations on intrinsic properties like thermal properties and dielectric properties (dielectric constant, dielectric loss and tanloss). The chief aim of current work is to improve the dielectric properties and study its possible use in high-frequency devices fabrication.

## 2. Experimental work

Replacement in the lithium nickel spinel ferrites was done by chemical method. In which LiNi<sub>0.5</sub>Fe<sub>2</sub>O<sub>4</sub> spinel ferrites were synthesized with the different molar concentration of Praseodymium adopting microemulsion chemical route [16, 17]. The standard available chemicals were used, its details is as follow: Sigma-Aldrich made Pr (NO<sub>3</sub>)<sub>3</sub>.6H<sub>2</sub>O (99.9% pure) Merk-Germany made Fe(NO<sub>3</sub>)<sub>2</sub>.9H<sub>2</sub>O (99% pure), Bio Basic-Canada made CTAB (Cetyl trimethylammonium bromide, 99% pure), BDH made NiCl<sub>2</sub>.6H<sub>2</sub>O (99% pure), and BDH made aqueous NH<sub>3</sub>(35% concentrated). Distilled water was used to prepare all solutions. Lithium, nickel and praseodymium salts were dissolved in distilled water to prepare 0.1molar solution. While ferric salt is dissolved in water to prepare 0.2M solution. Only CTAB was dissolved to have 0.3M solution. Solutions were distributed according to calculated volume and mixed while stirring on temperature controlled hotplate. On achieving 55°C of temperature, heating was stopped and CTAB solution was mixed. The pH of the mixture was 3. Diluted ammonia in distilled water was added to solution to achieve pH to 10. After attaining required pH the solution was further stirred for 5hr. During maintaining pH precipitates of Iron oxide settled down. These iron oxide precipitates were further washed to have a neutral solution. These precipitate then dried and ground to have the powder form of the samples. Some powder collected separately for TGA analysis whereas all these samples were annealed at 950°C. Then samples in powder form were analyzed with various techniques [18].

### 3. Results and discussion

The  $\text{Pr}^{+3}$  substituted LiNi-spinel nano ferrites were prepared by microemulsion route and were characterized by TGA, X-ray diffraction, Fourier transform IR, dielectric behavior and magnetic M-H loop etc. The synthesis and characterization of “ $\text{LiNi}_{0.5}\text{Pr}_x\text{Fe}_{2-x}\text{O}_4$ ” ( $x = 0.00$  to  $0.175$ ) ferrites have been described in detail in our previous communication (<https://doi.org/10.1016/j.ceramint.2017.07.228>), where crystalline size was in nano range [19]. Other analyses like TGA/DTA and dielectric studies for various samples are depicted here.

#### 3.1 TGA – DTA– DSC analysis

TGA, DTA, and DSC graphs of  $\text{LiNi}_{0.5}\text{Pr}_{0.07}\text{Fe}_{1.97}\text{O}_4$  ferrite was elaborated as shown in Fig. 1. The fabrication process, decomposition and annealing temperature was deduced from these characteristics curves. There were various stages of decompositions. These stages were observed from the trends of curves. DTA and DSC peaks were related to weight loss. Almost 12 % weight loss was found at temperature  $146.8^\circ\text{C}$ . This weight loss was attributed due to the decompositions, oxidation of organic materials and desertion of water present in samples [20, 21]. A further weight loss continued and reached 20% at temperature  $310.3^\circ\text{C}$ , which was related to the decompositions of organic materials and crystalline water present in nitrates precursor. Moreover, 22% weight loss was also found at the  $710.7^\circ\text{C}$  temperature which is suitable for the phase formation process in crystal structure [22]. No appreciable weight loss was found beyond  $850^\circ\text{C}$  which related to the formation of spinel phase in the crystal at this suitable temperature [23]. Two exothermic peaks were experienced at  $266.5^\circ\text{C}$  and  $613.6^\circ\text{C}$ . These peaks revealed the indications of remaining components such as chloride and nitrates in the samples. From TGA curve it is clear there is no weight loss in the range  $752\text{--}1000^\circ\text{C}$  which is an evidence of nanocrystalline ferrites [24, 25]. A sharp exothermic peak was observed at temperature  $289.8^\circ\text{C}$  in DCS curve. These curves describe the decomposition procedure and range of temperature in the fabrication method. From these curvatures, it is observed that decomposition was being taken in numerous stages. So spinel ferrite phase is exclusively formed and ignited satisfactory. Hence, no further calcination process is mandatory beyond  $950^\circ\text{C}$ .

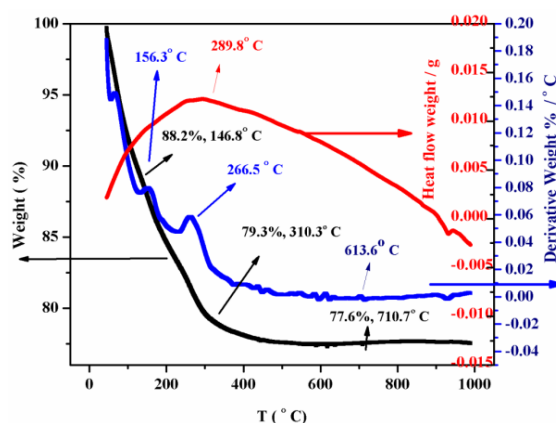


Fig. 1. TGA/DTA curves of “ $\text{LiNi}_{0.5}\text{Pr}_{0.07}\text{Fe}_{1.97}\text{O}_4$ ” spinel ferrite. ( $x=0.0$  to  $0.175$ ).

#### 3.2 Fourier transform infrared (FTIR) analysis

FTIR spectroscopy was employed for the confirmation of the spinel phase formation in all samples of “ $\text{LiNi}_{0.5}\text{Pr}_x\text{Fe}_{2-x}\text{O}_4$ ” ferrites with different concentration. These IR spectra were traced in the range  $400\text{--}1000\text{cm}^{-1}$ . There were two fundamental absorption band spectra present in the range from  $400$  to  $1000\text{cm}^{-1}$  analogous to the tetrahedral and octahedral complexes respectively [26]. These were named as  $\nu_1$  at around  $600\text{cm}^{-1}$  is high frequency band and  $\nu_2$  at around  $400\text{cm}^{-1}$

low-frequency band and these bands be the uniqueness of spinel phase structure [27]. The FTIR band in the range of  $400\text{-}1000\text{cm}^{-1}$  were exhibited in Fig. 2. The band arrangement change as the function of Pr contents and these values were tabulated in Table 1. The variation in  $\nu_2$  was from  $442$  to  $450\text{cm}^{-1}$  and that of  $\nu_1$  from  $550$  to  $561\text{cm}^{-1}$  [25, 28]. In ferrite spectra, the intrinsic vibrations on the tetrahedral groups a sharp absorption band was observed around  $600\text{cm}^{-1}$  and other band correspond to the octahedral groups. So the lattice constant variations resulted a minor shifting of  $\nu_1$  and  $\nu_2$  with increasing of praseodymium contents towards elevated frequency bands. This transformation in the lattice parameter affects the  $\text{Fe}^{3+}\text{-O}^{2-}$  enlarging vibrations which resulted an alteration in band situation [29, 30]. This disparity in the band position was projected as the difference in the  $\text{Fe}^{3+}\text{-O}^{2-}$  distance for the “octahedral and tetrahedral” compounds. Whereas cation allocation with tetrahedral sites and octahedral in spinel ferrite was detected from  $\nu_1$  and  $\nu_2$  frequency bands [31]. Generally Fe-O bond itself towards B-site. In the present spectra, It can be observed from spectra on the incorporation Pr content these octahedral peaks somewhat shift to higher values. Whereas on Pr content introduction, the tetrahedral incorporation peaks were somewhat shifted towards the lower frequency side. There are many peaks above the  $1000\text{cm}^{-1}$  these peaks are owing to H-O-H (water) stretching vibrations of trapped water [32].

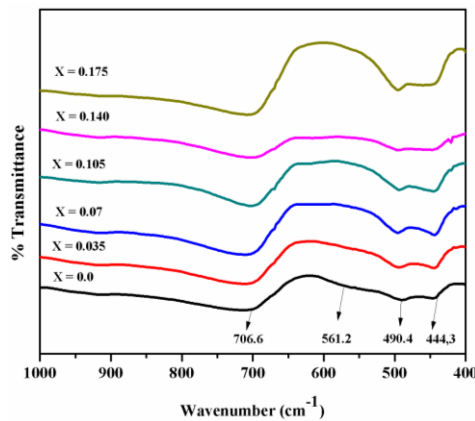


Fig. 2. FTIR spectra of “ $\text{LiNi}_{0.5}\text{Pr}_x\text{Fe}_{2-x}\text{O}_4$ ” spinel ferrites ( $x=0.0$  to  $0.175$ ) annealed at  $950\text{ }^\circ\text{C}$ .

### 3.3 Dielectric measurements

The dielectric characterization is one the application study of the given material. Especially this study was one of the important properties, particularly for ferrites to illuminate their appropriateness as high frequency device use. The structural parameter like composition and cation arrangement in the unit cell also affect these properties. Dielectrics properties also depend upon the method of preparation. Dielectric factor such as dielectric loss, complex dielectric constant and dielectric constant of “ $\text{LiNi}_{0.5}\text{Pr}_x\text{Fe}_{2-x}\text{O}_4$ ” ( $x$  between  $0.00$  and  $0.175$ ) ferrites were explored for frequency range  $1\text{MHz}$  to  $3\text{GHz}$  at standard temperature and pressure. The deviation in the dielectric constant (real and complex part) and tan loss with vibrating electric field was described in Fig. 3, 4 and 5. The variation in dielectric constant with reverence to frequency and Pr content was examined as follow. Table 2 showed both complex part and real of the dielectric constant and dielectric loss at some selected frequencies. That decreased when praseodymium content was increased. In ferrites materials polarization mechanism both  $\text{Fe}^{3+}$  and  $\text{Fe}^{2+}$  ions play an imperative function. However ferrous ( $\text{Fe}^{2+}$ ) ion play significant function during polarization and conduction process. Praseodymium ion ( $\text{Pr}^{3+}$ ) having larger ionic radii ions ware settled on octahedral sites [33, 34]. So as result of increasing concentration of praseodymium the iron content decreases, resulting a decrease in of iron ions who elucidate the drop in dielectric constant values [35-37]. Due to the occurrence of the second phase at a higher concentration of praseodymium the ferrous ions decreases, due to which as consequence electron substitute mechanism among ferrous and ferric ions was distressed or deferred. As a result polarization and after that dielectric constant

values decreased with praseodymium contents. Additionally, there was a prominent connection between the hopping “conduction mechanism” and also the dielectric performance of ferrites [34, 38, 39].

Table 1. FTIR absorption bands for “ $\text{LiNi}_{0.5}\text{Pr}_x\text{Fe}_{2-x}\text{O}_4$ ” spinel ferrites ( $x=0.0$  to  $0.175$ ).

S. No	Composition	$\nu_1$ ( $\text{cm}^{-1}$ )	$\nu_2$ ( $\text{cm}^{-1}$ )
1	$\text{LiNi}_{0.5}\text{Fe}_2\text{O}_4$	561	444
2	$\text{LiNi}_{0.5}\text{Pr}_{0.035}\text{Fe}_{1.965}\text{O}_4$	558	442
3	$\text{LiNi}_{0.5}\text{Pr}_{0.070}\text{Fe}_{1.93}\text{O}_4$	552	443
4	$\text{LiNi}_{0.5}\text{Pr}_{0.105}\text{Fe}_{1.895}\text{O}_4$	550	445
5	$\text{LiNi}_{0.5}\text{Pr}_{0.140}\text{Fe}_{1.86}\text{O}_4$	559	445
6	$\text{LiNi}_{0.5}\text{Pr}_{0.175}\text{Fe}_{1.825}\text{O}_4$	556	450

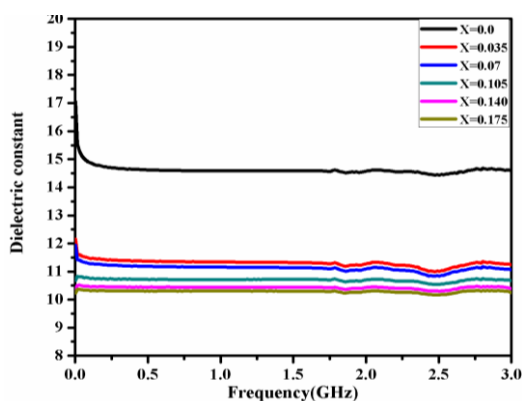


Fig. 3. Effect of frequency on the dielectric constant (real part) of “ $\text{LiNi}_{0.5}\text{Pr}_x\text{Fe}_{2-x}\text{O}_4$ ” spinel ferrites ( $x=0.0$  to  $0.175$ ).

Fig. 3 and 4 displayed that at hand is scattering in dielectric parameters with increasing frequency up to 3GHz. At 1MHz frequencies, the dielectric constants values decreased. Though in the GHz frequency region these values become very minutes. Some relaxation peaks were also observed at higher frequencies.

Table 2. Various dielectric parameters for “ $\text{LiNi}_{0.5}\text{Pr}_x\text{Fe}_{2-x}\text{O}_4$ ” spinel ferrites ( $x=0.0$  to  $0.175$ ).

Parameters	Frequency	$x=0$	$x=0.035$	$x=0.070$	$x=0.105$	$x=0.140$	$x=0.175$
Dielectric Constant	15 MHz	15.539	11.612	11.417	10.824	10.509	10.366
	1.0 GHz	14.587	11.338	11.156	10.715	10.445	10.305
	3.0 GHz	14.587	11.234	11.056	10.669	10.389	10.252
Dielectric Loss	15 MHz	4.468	2.870	2.205	1.914	1.613	1.473
	1.0 GHz	3.483	1.934	1.723	1.836	1.571	1.431
	3.0 GHz	3.484	1.935	1.700	1.787	1.501	1.364
$\tan\delta$	15 MHz	673.808	606.428	285.493	89.414	132.595	120.541
	1.0 GHz	3.372	3.035	2.853	1.642	1.187	1.079
	3.0 GHz	1.079	0.971	0.363	0.358	0.319	0.290

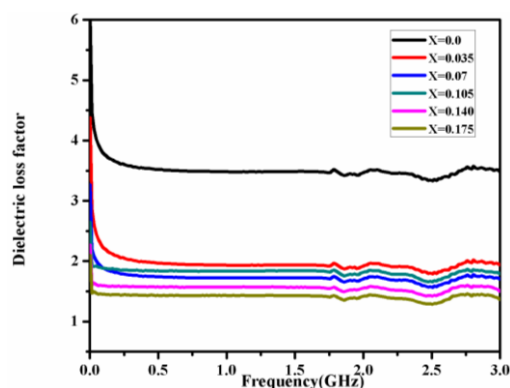


Fig. 4. Effect of frequency on the dielectric constant (imaginary part) of “ $\text{LiNi}_{0.5}\text{Pr}_x\text{Fe}_{2-x}\text{O}_4$ ” spinel ferrites ( $x=0.0$  to  $0.175$ ).

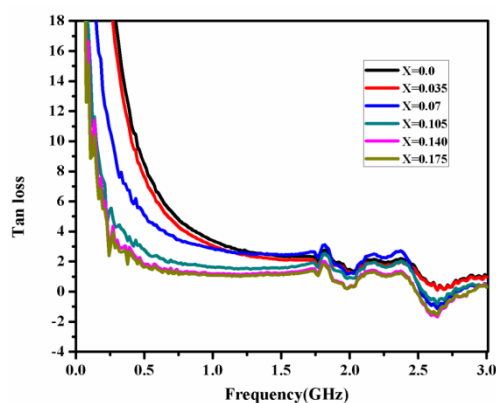


Fig. 5. Effect of frequency on the dielectric loss of “ $\text{LiNi}_{0.5}\text{Pr}_x\text{Fe}_{2-x}\text{O}_4$ ” spinel ferrites ( $x=0.0$  to  $0.175$ ).

This diffusion at the lower frequency region is a result of the space charge distribution. At the GHz frequency, two relaxation peaks around 2GHz and 2.5GHz are experienced. These peaks are the famous Debye-type relaxation justification model that was experienced while the jumping frequency of the  $\text{Fe}^{2+}$  and  $\text{Fe}^{3+}$  ions produced resonance. This resonance is due to coinciding of electron frequency with applied field frequency [40]. So at GHz frequencies region, these relaxation peaks were appropriate to the resonance of applied ac field with electrons [39, 41]. The dielectric scattering performance in ferrites is able to elucidate with the help of Maxwell–Wagner model and Koop’s phenomenological theory [42, 43].

As shown in Fig. 5 the deviation of tan loss by increasing frequency and the Pr molar concentration was revealed. Variation of tan loss was also observed like other parameters as frequency increased, tan loss decreased [44]. On the application of ac field with higher frequencies, the hopping frequency of the electron substitute between  $\text{Fe}^{2+}$  and  $\text{Fe}^{3+}$  ions could not trail the applied ac field further than certain decisive frequency and the loss was least.

#### 4. Conclusions

Praseodymium replacement in lithium ferrites were successfully prepared by facile microemulsion routine. Thermal analysis revealed material loss at different temperature and also confirmed the annealing temperature  $950^\circ\text{C}$ . FTIR group were experienced near  $400\text{cm}^{-1}$  and  $600\text{cm}^{-1}$  which revealed the typical features of the spinel structure. Dielectric studies were investigated for vibrating applied ac field from 1MHz to 3GHz frequency range. The dielectric factors were observed to decrease with the increase in Praseodymium concentrations and the very

small dielectric loss  $\sim 1.43$  for  $x = 0.175$  was observed. The inspected dielectric studies of parameters proposed the probable use of this kind of nano ferrites in high frequency devices applications.

### Acknowledgement

We are thankful to Balochistan University of Information Technology, Engineering and Management Sciences (BUIITEMS), Quetta Pakistan and The Islamia University of Bahawalpur providing necessary facilities.

### References

- [1] M. Ahmed, S. T. Bishay, F. Radwan, *Journal of Physics and Chemistry of Solids* **63**, 279 (2002).
- [2] V. Verma, R. Kotnala, V. Pandey, P. Kothari, L. Radhapiyari, B. Matheru, *Journal of Alloys and Compounds* **466**, 404 (2008).
- [3] M. Chaudhari, R. Kadam, S. Shelke, S. E. Shirsath, A. Kadam, D. Mane, *Powder Technology* **259**, 14 (2014).
- [4] I. Soibam, S. Phanjoubam, H. Sharma, H. Sarma, R. Laishram, C. Prakash, *Solid State Communications* **148**, 399 (2008).
- [5] M. F. Al-Hilli, S. Li, K. S. Kassim, *Journal of Magnetism and Magnetic Materials* **324**, 873 (2012).
- [6] J. Jing, L. Liangchao, X. Feng, *Journal of Rare Earths* **25**, 79 (2007).
- [7] M. Ahmed, S. T. Bishay, *Journal of Physics and Chemistry of Solids* **64**, 769 (2003).
- [8] C. Sun, K. Sun, *Solid State Communications* **141**, 258 (2007).
- [9] M. F. Al-Hilli, S. Li, K. S. Kassim, *Materials Chemistry and Physics* **128**, 127 (2011).
- [10] I. Betancourt, H. A. Davies, *Journal of Magnetism and Magnetic Materials* **261**, 328 (2003).
- [11] H.-X. Mai, Y.-W. Zhang, R. Si, Z.-G. Yan, L.-d. Sun, L.-P. You, C.-H. Yan, *Journal of the American Chemical Society* **128**, 6426 (2006).
- [12] J. Rodriguez-Carvajal, M. Fernandez-Diaz, J. Martinez, *Journal of Physics: Condensed Matter* **3**, 3215 (1991).
- [13] I. Ganesh, R. Johnson, G. V. N. Rao, Y. R. Mahajan, S. S. Madavendra, B. M. Reddy, *Ceramics International* **31**, 67 (2005).
- [14] V. L. Mathe, R. B. Kamble, *Materials Research Bulletin* **43**, 2160 (2008).
- [15] P. Dutta, M. Seehra, S. Thota, J. Kumar, *Journal of Physics: Condensed Matter* **20**, 015218 (2007).
- [16] S. Kumar, V. Singh, S. Aggarwal, U. K. Mandal, R. K. Kotnala, *Materials Science and Engineering: B*, **166**, 76 (2010).
- [17] R. Ali, M.A. Khan, A. Mahmood, A. H. Chughtai, A. Sultan, M. Shahid, M. Ishaq, M. F. Warsi, *Ceramics International* **40**, 3841 (2014).
- [18] Z. A. Gilani, M. F. Warsi, M. N. Anjum, I. Shakir, S. Naseem, S. Riaz, M. A. Khan, *Journal of Alloys and Compounds* **639**, 268 (2015).
- [19] R. Ali, M.A. Khan, A. Manzoor, M. Shahid, S. Haider, A. S. Malik, M. Sher, I. Shakir, M. Farooq Warsi, *Journal of Magnetism and Magnetic Materials* **429**, 142 (2017).
- [20] C. Sun, K. Sun, *Physica B: Condensed Matter* **391**, 335 (2007).
- [21] A. M. Abo El Ata, S. M. Attia, D. El Kony, A. H. Al-Hammadi, *Journal of Magnetism and Magnetic Materials* **295**, 28 (2005).
- [22] M. Azhar Khan, M. Sabir, A. Mahmood, M. Asghar, K. Mahmood, M. Afzal Khan, I. Ahmad, M. Sher, M. Farooq Warsi, *Journal of Magnetism and Magnetic Materials* **360**, 188 (2014).
- [23] M. Azhar Khan, M. Sabir, A. Mahmood, M. Asghar, K. Mahmood, M. Afzal Khan, I. Ahmad, M. Sher, M. Farooq Warsi, *Journal of Magnetism and Magnetic Materials* **360**, 188 (2014).
- [24] M. Asif Iqbal, M.-U. Islam, M. N. Ashiq, I. Ali, A. Iftikhar, H. M. Khan, *Journal of Alloys and Compounds* **579**, 181 (2013).

- [25] A. Manzoor, M. A. Khan, M. Y. Khan, M. N. Akhtar, A. Hussain, *Ceramics International* **44**, 6321 (2018).
- [26] A. I. Ali, M. A. Ahmed, N. Okasha, M. Hammam, J. Y. Son, *Journal of Materials Research and Technology* **2**, 356 (2013).
- [27] A. Ghasemi, M. Mousavinia, *Ceramics International* **40**, 2825 (2014).
- [28] S. T. Assar, H. F. Abosheisha, S. A. Saafan, M. K. El Nimr, *Journal of Molecular Structure*, **1084**, 128 (2015).
- [29] C. Choodamani, G. P. Nagabhushana, S. Ashoka, B. Daruka Prasad, B. Rudraswamy, G. T. Chandruppa, *Journal of Alloys and Compounds* **578**, 103 (2013).
- [30] B. J. S. N., J. R., *Materials Letters* **81**, 52 (2012).
- [31] S. Amiri, H. Shokrollahi, *Journal of Magnetism and Magnetic Materials* **345**, 18 (2013).
- [32] Z. Karimi, Y. Mohammadifar, H. Shokrollahi, S. K. Asl, G. Yousefi, L. Karimi, *Journal of Magnetism and Magnetic Materials* **361**, 150 (2014).
- [33] R. Parvin, A. A. Momin, A. K. M. A. Hossain, *Journal of Magnetism and Magnetic Materials*, **401**, 760 (2016).
- [34] A. P. Surzhikov, A. V. Malyshev, E. N. Lysenko, V. A. Vlasov, A. N. Sokolovskiy, *Ceramics International* **43**, 9778 (2017).
- [35] D. Ravinder, A. Chandrashekhara Reddy, *Materials Letters* **57**, 2855 (2003).
- [36] M. F. Al-Hilli, S. Li, K. S. Kassim, *Materials Chemistry and Physics* **128**, 127 (2011).
- [37] M. Abdullah Dar, K. Majid, K. M. Batoo, R. K. Kotnala, *Journal of Alloys and Compounds*, **632**, 307 (2015).
- [38] P. P. Hankare, R. P. Patil, U. B. Sankpal, S. D. Jadhav, I. S. Mulla, K. M. Jadhav, B. K. Chougule, *Journal of Magnetism and Magnetic Materials* **321**, 3270 (2009).
- [39] R. Ali, A. Mahmood, M. A. Khan, A. H. Chughtai, M. Shahid, I. Shakir, M. F. Warsi, *Journal of Alloys and Compounds* **584**, 363 (2014).
- [40] J. H. Joshi, D. K. Kanchan, M. J. Joshi, H. O. Jethva, K. D. Parikh, *Materials Research Bulletin* **93**, 63 (2017).
- [41] M. A. Khan, M. U. Islam, M. Ishaque, I. Z. Rahman, *Journal of Alloys and Compounds* **519**, 156 (2012).
- [42] B. Ramesh, D. Ravinder, *Materials Letters* **62**, 2043 (2008).
- [43] S. C. Watawe, U. A. Bamne, S. P. Gonbare, R. B. Tangsali, *Materials Chemistry and Physics* **103**, 323 (2007).
- [44] M. Younis, M. Saleem, S. Atiq, S. Naseem, *Ceramics International*, (2018).